Event-wise (Pt) fluctuations in Au-Au collisions at root sNN=130 GeV

J. Adams, C. Adler, M. M. Aggarwal, Z. Ahammed, J. Amonett, B. D. Anderson, M. Anderson, D. Arkhipkin, G. S. Averichev, S. K. Badyal, J. Balewski, O. Barannikova, L. S. Barnby, J. Baudot, S. Bekele, V. V. Belaga, R. Bellwied, J. Berger, B. I. Bezverkhny, S. Bhardwaj, P. Bhaskar, A. K. Bhati, H. Bichsel, A. Billmeier, L. C. Bland, C. O. Blyth, B. E. Bonner, M. Botje, A. Boucham, A. Brandin, A. Bravar, R. V. Cadman, X. Z. Cai, H. Caines, M. C. D. Sanchez, J. Carroll, J. Castillo, M. Castro, D. Cebra, P. Chaloupka, S. Chattopadhyay, H. F. Chen, Y. Chen, S. P. Chernenko, M. Cherney, A. Chikanian, B. Choi, W. Christie, J. P. Coffin, T. M. Cormier, J. G. Cramer, H. J. Crawford, D. Das, S. Das, A. A. Derevschikov, L. Didenko, T. Dietel, X. Dong, J. E. Draper, F. Du, A. K. Dubey, V. B. Dunin, J. C. Dunlop, M. R. D. Majumdar, V. Eckardt, L. G. Efimov, V. Emelianov, J. Engelage, G. Eppley, B. Erazmus, M. Estienne, P. Fachini, V. Faine, J. Faivre, R. Fatemi, K. Filimonov, P. Filip, E. Finch, Y. Fisyak, D. Flierl, K. J. Foley, J. Fu, C. A. Gagliardi, M. S. Ganti, T. D. Gutierrez, N. Gagunashvili, J. Gans, L. Gaudichet, M. Germain, F. Geurts, V. Ghazikhanian, P. Ghosh, J. E. Gonzalez, O. Grachov, V. Grigoriev, S. Gronstal, D. Grosnick, M. Guedon, S. M. Guertin, A. Gupta, E. Gushin, T. J. Hallman, D. Hardtke, J. W. Harris, M. Heinz, T. W. Henry, S. Heppelmann, T. Herston, B. Hippolyte, A. Hirsch, E. Hjort, G. W. Hoffmann, M. Horsley, H. Z. Huang, S. L. Huang, T. J. Humanic, G. Igo, A. Ishihara, P. Jacobs, W. W. Jacobs, M. Janik, I. Johnson, P. G. Jones, E. G. Judd, S. Kabana, M. Kaneta, M. Kaplan, D. Keane, J. Kiryluk, A. Kisiel, J. Klay, S. R. Klein, A. Klyachko, D. D. Koetke, T. Kollegger, A. S. Konstantinov, M. Kopytine, L. Kotchenda, A. D. Kovalenko, M. Kramer, P. Kravtsov, K. Krueger, C. Kuhn, A. I. Kulikov, A. Kumar, G. J. Kunde, C. L. Kunz, R. K. Kutuev, A. A. Kuznetsov, M. A. C. Lamont, J. M. Landgraf, S. Lange, C. P. Lansdell, B. Lasiuk, F. Laue, J. Lauret, A. Lebedev, R. Lednicky, V. M. Leontiev, M. J. LeVine, C. Li, Q. Li, S. J. Lindenbaum, M. A. Lisa, F. Liu, L. Liu, Z. Liu, Q. J. Liu, T. Ljubicic, W. J. Llope, H. Long, R. S. Longacre, M. Lopez-Noriega, W. A. Love, T. Ludlam, D. Lynn, J. Ma, Y. G. Ma, D. Magestro, S. Mahajan, L. K. Mangotra, D. P. Mahapatra, R. Majka, R. Manweiler, S. Margetis, C. Markert, L. Martin, J. Marx, H. S. Matis, Y. A. Matulenko, T. S. McShane, F. Meissner, Y. Melnick, A. Meschanin, M.

Messer, M. L. Miller, Z. Milosevich, N. G. Minaev, C. Mironov, D. Mishra, J. Mitchell, B. Mohanty, L. Molnar, C. F. Moore, M. J. Mora-Corral, V. Morozov, M. M. de Moura, M. G. Munhoz, B. K. Nandi, S. K. Nayak, T. K. Nayak, J. M. Nelson, P. Nevski, V. A. Nikitin, L. V. Nogach, B. Norman, S. B. Nurushev, G. Odyniec, A. Ogawa, V. Okorokov, M. Oldenburg, D. Olson, G. Paic, S. U. Pandey, S. K. Pal, Y. Panebratsev, S. Y. Panitkin, A. I. Pavlinov, T. Pawlak, V. Perevoztchikov, W. Peryt, V. A. Petrov, S. C. Phatak, R. Picha, M. Planinic, J. Pluta, N. Porile, J. Porter, A. M. Poskanzer, M. Potekhin, E. Potrebenikova, B. V. K. S. Potukuchi, D. Prindle, C. Pruneau, J. Putschke, G. Rai, G. Rakness, R. Raniwala, S. Raniwala, O. Ravel, R. L. Ray, S. V. Razin, D. Reichhold, J. G. Reid, G. Renault, F. Retiere, A. Ridiger, H. G. Ritter, J. B. Roberts, O. V. Rogachevski, J. L. Romero, A. Rose, C. Roy, L. J. Ruan, R. Sahoo, I. Sakrejda, S. Salur, J. Sandweiss, I. Savin, J. Schambach, R. P. Scharenberg, N. Schmitz, L. S. Schroeder, K. Schweda, J. Seger, D. Seliverstov, P. Seyboth, E. Shahaliev, M. Shao, M. Sharma, K. E. Shestermanov, S. S. Shimanskii, R. N. Singaraju, F. Simon, G. Skoro, N. Smirnov, R. Snellings, G. Sood, P. Sorensen, J. Sowinski, H. M. Spinka, B. Srivastava, S. Stanislaus, R. Stock, A. Stolpovsky, M. Strikhanov, B. Stringfellow, C. Struck, A. A. P. Suaide, E. Sugarbaker, C. Suire, M. Sumbera, B. Surrow, T. J. M. Symons, A. S. de Toledo, P. Szarwas, A. Tai, J. Takahashi, A. H. Tang, D. Thein, J. H. Thomas, V. Tikhomirov, M. Tokarev, M. B. Tonjes, T. A. Trainor, S. Trentalange, R. E. Tribble, M. D. Trivedi, V. Trofimov, O. Tsai, T. Ullrich, D. G. Underwood, G. V. Buren, A. M. VanderMolen, A. N. Vasiliev, M. Vasiliev, S. E. Vigdor, Y. P. Viyogi, W. Waggoner, F. Wang, G. Wang, X. L. Wang, Z. M. Wang, H. Ward, J. W. Watson, R. Wells, G. D. Westfall, C. Whitten, H. Wieman, R. Willson, S. W. Wissink, R. Witt, J. Wood, J. Wu, N. Xu, Z. Xu, Z. Z. Xu, A. E. Yakutin, E. Yamamoto, J. Yang, P. Yepes, V. I. Yurevich, Y. V. Zanevski, I. Zborovsky, H. Zhang, H. Y. Zhang, W. M. Zhang, Z. P. Zhang, P. A. Zolnierczuk, R. Zoulkarneev, J. Zoulkarneeva, and A. N. Zubarev

Event-wise $\langle p_t \rangle$ fluctuations in Au-Au collisions at $\sqrt{s_{NN}} = 130$ GeV

J. Adams,[3] C. Adler,[12] M. M. Aggarwal,[25] Z. Ahammed,[28] J. Amonett,[17] B. D. Anderson,[17] M. Anderson,[5] D. Arkhipkin,[11]
G. S. Averichev,[10] S. K. Badyal,[16] J. Balewski,[13] O. Barannikova,[28,10] L. S. Barnby,[17] J. Baudot,[15] S. Bekele,[24] V. V. Belaga,[10]
R. Bellwied,[41] J. Berger,[12] B. I. Bezverkhny,[43] S. Bhardwaj,[29] P. Bhaskar,[38] A. K. Bhati,[25] H. Bichsel,[40] A. Billmeier,[41]
L. C. Bland,[2] C. O. Blyth,[3] B. E. Bonner,[30] M. Botje,[23] A. Boucham,[34] A. Brandin,[21] A. Bravar,[2] R. V. Cadman,[1] X. Z. Cai,[33]
H. Caines,[43] M. Calderón de la Barca Sánchez,[2] J. Carroll,[18] J. Castillo,[18] M. Castro,[41] D. Cebra,[45] P. Chaloupka,[9]
S. Chattopadhyay,[38] H. F. Chen,[32] Y. Chen,[6] S. P. Chernenko,[10] M. Cherney,[8] A. Chikanian,[43] B. Choi,[36] W. Christie,[2]
J. P. Coffin,[15] T. M. Cormier,[41] J. G. Cramer,[40] H. J. Crawford,[4] D. Das,[38] S. Das,[38] A. A. Derevschikov,[27] L. Didenko,[2]
T. Dietel,[12] X. Dong,[32,18] J. E. Draper,[5] F. Du,[43] A. K. Dubey,[14] V. B. Dunin,[10] J. C. Dunlop,[2] M. R. Dutta Majumdar,[38]
V. Eckardt,[19] L. G. Efimov,[10] V. Emelianov,[21] J. Engelage,[4] G. Eppley,[30] B. Erazmus,[34] M. Estienne,[34] P. Fachini,[2] V. Faine,[2]
J. Faivre,[15] R. Fatemi,[13] K. Filimonov,[18] P. Filip,[9] E. Finch,[43] Y. Fisyak,[2] D. Flierl,[12] K. J. Foley,[2] J. Fu,[42] C. A. Gagliardi,[35]
M. S. Ganti,[38] T. D. Gutierrez,[5] N. Gagunashvili,[10] J. Gans,[43] L. Gaudichet,[34] M. Germain,[15] F. Geurts,[30] V. Ghazikhanian,[6]
P. Ghosh,[38] J. E. Gonzalez,[6] O. Grachov,[41] V. Grigoriev,[21] S. Gronstal,[8] D. Grosnick,[37] M. Guedon,[15] S. M. Guertin,[6]
A. Gupta,[16] E. Gushin,[21] T. J. Hallman,[2] D. Hardtke,[18] J. W. Harris,[43] M. Heinz,[43] T. W. Henry,[35] S. Heppelmann,[26]
T. Herston,[28] B. Hippolyte,[43] A. Hirsch,[28] E. Hjort,[18] G. W. Hoffmann,[36] M. Horsley,[43] H. Z. Huang,[6] S. L. Huang,[32]
T. J. Humanic,[24] G. Igo,[6] A. Ishihara,[36] P. Jacobs,[18] W. W. Jacobs,[13] M. Janik,[39] I. Johnson,[18] P. G. Jones,[3] E. G. Judd,[4]
S. Kabana,[43] M. Kaneta,[18] M. Kaplan,[7] D. Keane,[17] J. Kiryluk,[6] A. Kisiel,[39] J. Klay,[18] S. R. Klein,[18] A. Klyachko,[13]
D. D. Koetke,[37] T. Kollegger,[12] A. S. Konstantinov,[27] M. Kopytine,[17] L. Kotchenda,[21] A. D. Kovalenko,[10] M. Kramer,[22]
P. Kravtsov,[21] K. Krueger,[1] C. Kuhn,[15] A. I. Kulikov,[10] A. Kumar,[25] G. J. Kunde,[43] C. L. Kunz,[7] R. Kh. Kutuev,[11]
A. A. Kuznetsov,[10] M. A. C. Lamont,[3] J. M. Landgraf,[2] S. Lange,[12] C. P. Lansdell,[36] B. Lasiuk,[43] F. Laue,[2] J. Lauret,[2]
A. Lebedev,[2] R. Lednický,[10] V. M. Leontiev,[27] M. J. LeVine,[2] C. Li,[32] Q. Li,[41] S. J. Lindenbaum,[22] M. A. Lisa,[24] F. Liu,[42]
L. Liu,[42] Z. Liu,[42] Q. J. Liu,[40] T. Ljubicic,[2] W. J. Llope,[30] H. Long,[6] R. S. Longacre,[2] M. Lopez-Noriega,[24] W. A. Love,[2]
T. Ludlam,[2] D. Lynn,[2] J. Ma,[46] Y. G. Ma,[33] D. Magestro,[24] S. Mahajan,[16] L. K. Mangotra,[16] D. P. Mahapatra,[14] R. Majka,[43]
R. Manweiler,[37] S. Margetis,[17] C. Markert,[43] L. Martin,[34] J. Marx,[18] H. S. Matis,[18] Yu. A. Matulenko,[27] T. S. McShane,[8]
F. Meissner,[18] Yu. Melnick,[27] A. Meschanin,[27] M. Messer,[2] M. L. Miller,[43] Z. Milosevich,[7] N. G. Minaev,[27] C. Mironov,[17]
D. Mishra,[14] J. Mitchell,[30] B. Mohanty,[38] L. Molnar,[28] C. F. Moore,[36] M. J. Mora-Corral,[19] V. Morozov,[18] M. M. de Moura,[41]
M. G. Munhoz,[31] B. K. Nandi,[38] S. K. Nayak,[16] T. K. Nayak,[38] J. M. Nelson,[3] P. Nevski,[2] V. A. Nikitin,[11] L. V. Nogach,[27]
B. Norman,[17] S. B. Nurushev,[27] G. Odyniec,[18] A. Ogawa,[2] V. Okorokov,[21] M. Oldenburg,[18] D. Olson,[18] G. Paic,[24]
S. U. Pandey,[41] S. K. Pal,[38] Y. Panebratsev,[47] S. Y. Panitkin,[2] A. I. Pavlinov,[41] T. Pawlak,[39] V. Perevoztchikov,[2] W. Peryt,[39]
V. A. Petrov,[11] S. C. Phatak,[14] R. Picha,[5] M. Planinic,[44] J. Pluta,[39] N. Porile,[28] J. Porter,[2] A. M. Poskanzer,[18] M. Potekhin,[2]
E. Potrebenikova,[10] B. V. K. S. Potukuchi,[16] D. Prindle,[40] C. Pruneau,[41] J. Putschke,[19] G. Rai,[18] G. Rakness,[13] R. Raniwala,[29]
S. Raniwala,[29] O. Ravel,[34] R. L. Ray,[36] S. V. Razin,[10,13] D. Reichhold,[28] J. G. Reid,[40] G. Renault,[34] F. Retiere,[18] A. Ridiger,[21]
H. G. Ritter,[18] J. B. Roberts,[30] O. V. Rogachevski,[10] J. L. Romero,[5] A. Rose,[41] C. Roy,[34] L. J. Ruan,[32,12] R. Sahoo,[14]
I. Sakrejda,[18] S. Salur,[43] J. Sandweiss,[43] I. Savin,[11] J. Schambach,[36] R. P. Scharenberg,[28] N. Schmitz,[19] L. S. Schroeder,[18]
K. Schweda,[18] J. Seger,[8] D. Seliverstov,[21] P. Seyboth,[19] E. Shahaliev,[10] M. Shao,[32] M. Sharma,[25] K. E. Shestermanov,[27]
S. S. Shimanskii,[10] R. N. Singaraju,[38] F. Simon,[19] G. Skoro,[10] N. Smirnov,[43] R. Snellings,[23] G. Sood,[25] P. Sorensen,[6]
J. Sowinski,[13] H. M. Spinka,[1] B. Srivastava,[28] S. Stanislaus,[37] R. Stock,[12] A. Stolpovsky,[41] M. Strikhanov,[21] B. Stringfellow,[28]
C. Struck,[12] A. A. P. Suaide,[41] E. Sugarbaker,[24] C. Suire,[2] M. Šumbera,[9] B. Surrow,[2] T. J. M. Symons,[18]
A. Szanto de Toledo,[31] P. Szarwas,[39] A. Tai,[6] J. Takahashi,[31] A. H. Tang,[2,23] D. Thein,[6] J. H. Thomas,[18] V. Tikhomirov,[21]
M. Tokarev,[10] M. B. Tonjes,[20] T. A. Trainor,[40] S. Trentalange,[6] R. E. Tribble,[35] M. D. Trivedi,[38] V. Trofimov,[21] O. Tsai,[6]
T. Ullrich,[2] D. G. Underwood,[1] G. Van Buren,[2] A. M. VanderMolen,[20] A. N. Vasiliev,[27] M. Vasiliev,[35] S. E. Vigdor,[13]
Y. P. Viyogi,[38] W. Waggoner,[8] F. Wang,[28] G. Wang,[17] X. L. Wang,[32] Z. M. Wang,[32] H. Ward,[36] J. W. Watson,[17] R. Wells,[24]
G. D. Westfall,[20] C. Whitten, Jr.,[6] H. Wieman,[18] R. Willson,[24] S. W. Wissink,[13] R. Witt,[43] J. Wood,[6] J. Wu,[32] N. Xu,[18] Z. Xu,[2]
Z. Z. Xu,[32] A. E. Yakutin,[27] E. Yamamoto,[18] J. Yang,[6] P. Yepes,[30] V. I. Yurevich,[10] Y. V. Zanevski,[10] I. Zborovský,[9]
H. Zhang,[43,2] H. Y. Zhang,[17] W. M. Zhang,[17] Z. P. Zhang,[32] P. A. Żołnierczuk,[13] R. Zoulkarneev,[11] J. Zoulkarneeva,[11] and
A. N. Zubarev[10]

(STAR Collaboration)

[1]*Argonne National Laboratory, Argonne, Illinois 60439, USA*
[2]*Brookhaven National Laboratory, Upton, New York 11973, USA*
[3]*University of Birmingham, Birmingham, United Kingdom*
[4]*University of California, Berkeley, California 94720, USA*
[5]*University of California, Davis, California 95616, USA*
[6]*University of California, Los Angeles, California 90095, USA*
[7]*Carnegie Mellon University, Pittsburgh, Pennsylvania 15213, USA*
[8]*Creighton University, Omaha, Nebraska 68178, USA*
[9]*Nuclear Physics Institute AS CR, Řež/Prague, Czech Republic*
[10]*Laboratory for High Energy (JINR), Dubna, Russia*

[11]*Particle Physics Laboratory (JINR), Dubna, Russia*
[12]*University of Frankfurt, Frankfurt, Germany*
[13]*Indiana University, Bloomington, Indiana 47408, USA*
[14]*Insitute of Physics, Bhubaneswar 751005, India*
[15]*Institut de Recherches Subatomiques, Strasbourg, France*
[16]*University of Jammu, Jammu 180001, India*
[17]*Kent State University, Kent, Ohio 44242, USA*
[18]*Lawrence Berkeley National Laboratory, Berkeley, California 94720, USA*
[19]*Max-Planck-Institut für Physik, Munich, Germany*
[20]*Michigan State University, East Lansing, Michigan 48824, USA*
[21]*Moscow Engineering Physics Institute, Moscow, Russia*
[22]*City College of New York, New York, New York 10031, USA*
[23]*NIKHEF, Amsterdam, The Netherlands*
[24]*Ohio State University, Columbus, Ohio 43210, USA*
[25]*Panjab University, Chandigarh 160014, India*
[26]*Pennsylvania State University, University Park, Pennsylvania 16802, USA*
[27]*Institute of High Energy Physics, Protvino, Russia*
[28]*Purdue University, West Lafayette, Indiana 47907, USA*
[29]*University of Rajasthan, Jaipur 302004, India*
[30]*Rice University, Houston, Texas 77251, USA*
[31]*Universidade de Sao Paulo, Sao Paulo, Brazil*
[32]*University of Science & Technology of China, Anhui 230027, China*
[33]*Shanghai Institute of Nuclear Research, Shanghai 201800, China*
[34]*SUBATECH, Nantes, France*
[35]*Texas A&M, College Station, Texas 77843, USA*
[36]*University of Texas, Austin, Texas 78712, USA*
[37]*Valparaiso University, Valparaiso, Indiana 46383, USA*
[38]*Variable Energy Cyclotron Centre, Kolkata 700064, India*
[39]*Warsaw University of Technology, Warsaw, Poland*
[40]*University of Washington, Seattle, Washington 98195, USA*
[41]*Wayne State University, Detroit, Michigan 48201, USA*
[42]*Institute of Particle Physics, CCNU (HZNU), Wuhan, 430079 China*
[43]*Yale University, New Haven, Connecticut 06520, USA*
[44]*University of Zagreb, HR-10002 Zagreb, Croatia*
[45]*University of California, Davis, California 95616, USA*
[46]*University of California, Los Angeles, California 90095, USA*
[47]*Laboratory for High Energy (JINR), Dubna, Russia*
[48]*Brookhaven National Laboratory, Upton, New York 11973, USA*

We present the first large-acceptance measurement of event-wise mean transverse momentum $\langle p_t \rangle$ fluctuations for Au-Au collisions at nucleon-nucleon center-of-momentum collision energy $\sqrt{s_{NN}} = 130$ GeV. The observed nonstatistical $\langle p_t \rangle$ fluctuations substantially exceed in magnitude fluctuations expected from the finite number of particles produced in a typical collision. The r.m.s. fractional width excess of the event-wise $\langle p_t \rangle$ distribution is 13.7 ± 0.1(stat) ± 1.3(syst)% relative to a statistical reference, for the 15% most-central collisions and for charged hadrons within pseudorapidity range $|\eta| < 1$, 2π azimuth, and $0.15 \leqslant p_t \leqslant 2$ GeV/c. The width excess varies smoothly but nonmonotonically with collision centrality and does not display rapid changes with centrality which might indicate the presence of critical fluctuations. The reported $\langle p_t \rangle$ fluctuation excess is qualitatively larger than those observed at lower energies and differs markedly from theoretical expectations. Contributions to $\langle p_t \rangle$ fluctuations from semihard parton scattering in the initial state and dissipation in the bulk colored medium are discussed.

I. INTRODUCTION

Fluctuation analysis of relativistic heavy ion collisions has been advocated to search for critical phenomena near the predicted hadron-parton phase boundary of quantum chromodynamics (QCD) [1–3]. Nonstatistical fluctuations (excess variance beyond statistical fluctuations due to finite particle number), varying rapidly with collision energy,

projectile size, or collision centrality and interpreted as critical fluctuations, could indicate a transition to a quark-gluon plasma [1–3]. Nonstatistical fluctuations could also appear in systems incompletely equilibrated following initial-state multiple scattering (Cronin effect [4] and minimum-bias hard parton scattering—minijets [5]), or as an aspect of fragmentation of color strings produced in nucleon-nucleon collisions or the bulk medium in *A-A* collisions. The study of nonstatistical fluctuations and the correlations that produce them is a central aspect of the Relativistic Heavy Ion Collider (RHIC) research program. The specific goal of the present work is to determine the magnitude and collision centrality dependence of nonstatistical fluctuations in momentum space at large momentum scales using the largest angular acceptance detector available at RHIC.

The dynamical representation of relativistic nuclear collisions can be separated into transverse (perpendicular to the beam axis) and longitudinal (parallel to the beam axis) phase spaces. In this paper, we focus on transverse phase space, including transverse momentum magnitude p_t and momentum azimuth angle ϕ, within relatively small pseudorapidity η intervals. Assuming rapid longitudinal (Bjorken) expansion of the collision system [6], separate η intervals can be treated as quasiindependent (causally disconnected) dynamical systems. In this analysis, we calculate the *event-wise mean transverse momentum* for each collision event within a detector kinematic acceptance

$$\langle p_t \rangle \equiv \frac{1}{N} \sum_{i=1}^{N} p_{t,i}, \qquad (1)$$

where i is a particle index and N represents the measured charged-particle multiplicity within the detector acceptance for a given collision event. Quantity $\langle p_t \rangle$ is monotonically related to the "temperature" of the event-wise p_t distribution, plus any collective transverse velocity of the collision system. The distribution of $\langle p_t \rangle$ over a collision event ensemble, especially any excess variance of this distribution beyond what is expected for purely statistical fluctuations, reflects the underlying dynamics and degree of equilibration of heavy ion collisions.

Some aspects of heavy ion collisions produce correlations/fluctuations that depend on the relative charge of a charged hadron pair [7–9], including quantum and Coulomb correlations [10], resonance decays, color-string fragmentation (e.g., charge ordering along the string axis [11,12]), and minijet fragmentation. Charge-dependent combinations for pion pairs can be directly related to isospin components. For nonidentified charged hadron pairs in the collisions studied here, which are dominated by pions but include other charged hadrons (e.g., protons, kaons, and their antiparticles), the relation to isospin remains useful but becomes approximate. To isolate the different isospin aspects of fluctuations and correlations we measure separately the like-sign (LS) and unlike-sign (US) charge-pair contributions and also form charge-independent (CI) and charge-dependent (CD) combinations, with CI = LS + US (approximately isoscalar) and CD = LS − US (approximately isovector), respectively.

In this paper, we report the first large-acceptance measurement of $\langle p_t \rangle$ fluctuations at RHIC using the STAR detector. Results are presented for unidentified charged hadrons using 183 000 (183k) central and 205 000 (205k) minimum-trigger-bias ensembles of Au-Au collision events at $\sqrt{s_{NN}} = 130$ GeV [center-of-momentum (CM) energy per nucleon-nucleon pair]. Experimental details and the observed $\langle p_t \rangle$ distribution for central events are presented in Secs. II–III. Quantities used to measure nonstatistical $\langle p_t \rangle$ fluctuations are discussed in Sec. IV and the Appendix. Results and discussion are presented in Secs. V–VIII; the observed large excess of $\langle p_t \rangle$ fluctuations at RHIC is compared to other measurements and to theoretical models, including hard parton scattering in the initial state and/or hadronic rescattering. Conclusions are presented in Sec. IX.

II. SUMMARY OF EXPERIMENT

Data for this analysis were obtained with the STAR detector [13] employing a 0.25 T uniform magnetic field parallel to the beam axis. Event triggering with the central trigger barrel (CTB) scintillators and zero-degree calorimeters (ZDC) and charged-particle kinematic measurements with the time projection chamber (TPC) are described in [13]. TPC tracking efficiency was determined to be 80–95% within $|\eta| < 1$ and $p_t > 200$ MeV/c by embedding simulated tracks in real-data events [14], and it was uniform in azimuth to 3% (r.m.s.) over 2π. Split-track removal required the fraction of valid space points used in a track fit relative to the maximum number possible to be $>50\%$. A primary event vertex within 75 cm of the axial center of the TPC was required. Valid TPC tracks fell within the full detector acceptance, defined here by $0.15 < p_t < 2.0$ GeV/c, $|\eta| < 1$, and 2π in azimuth. Primary tracks were defined as having a distance of closest approach less than 3 cm from the reconstructed primary vertex which included a large fraction of true primary hadrons plus approximately 7% background contamination [14].

Two data sets were analyzed: (1) 183k central triggered Au-Au collision events constituting the 15% most-central collisions as determined by scintillator hits in the STAR CTB and (2) 205k minimum-bias collision events triggered by ZDC coincidence. The latter events were divided into eight centrality classes based on TPC track multiplicity in $|\eta| \leqslant 0.5$ [14], the eight event classes comprising approximately equal fractions of the upper $87 \pm 2\%$ of the Au-Au total hadronic cross section.

III. MEAN p_t DISTRIBUTION

The frequency distribution of event-wise $\langle p_t \rangle$ for 183k or the 15% most-central collision events is first studied graphically. The data histogram is compared to a statistical reference distribution and is examined for evidence of anomalous event classes which could indicate either novel collision dynamics [1] or experimental anomalies. The event-wise $\langle p_t \rangle$ data distribution is shown as the histogram in the upper panel of Fig. 1. Those data, representing $80 \pm 5\%$ of the true primary
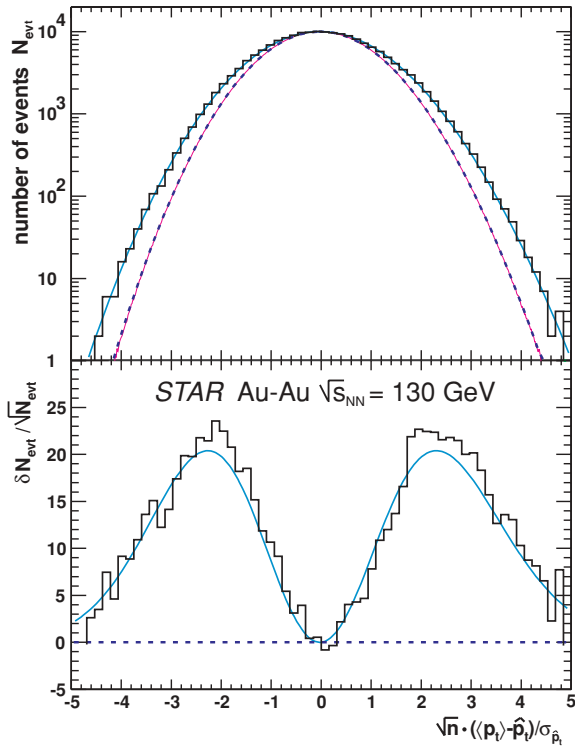
FIG. 1. (Color online) Upper panel: Event frequency distribution on $\sqrt{n}(\langle p_t \rangle - \hat{p}_t)/\sigma_{\hat{p}_t}$ (see text) for 80% of primary charged hadrons in $|\eta| < 1$ for 183k central events (histogram) compared to gamma reference (dashed curve), Monte Carlo reference (solid curve underlying gamma reference), and broadened distribution (solid curve underlying data, not a fit—see text). Lower panel: Difference in upper panel between data and gamma reference (histogram) or between broadened distribution and gamma reference (solid curve) normalized by the Poisson error $\sqrt{N_{\text{evt}}}$ in each bin.

particles within the acceptance, were binned using quantity $(\langle p_t \rangle - \hat{p}_t)/(\sigma_{\hat{p}_t}/\sqrt{n})$, where $\hat{p}_t$ and $\sigma_{\hat{p}_t}^2$ are, respectively, the mean and variance of the inclusive p_t distribution of all accepted particles in the event ensemble and n is the event-wise multiplicity within the defined acceptance. That choice of event-wise *random variable* rather than $\langle p_t \rangle$ is explained as follows.

For independent particle p_t samples from a fixed *parent* distribution (no nonstatistical fluctuations) the r.m.s. width of the frequency distribution on $\langle p_t \rangle$ is itself dependent on event multiplicity n as $\sigma_{\hat{p}_t}/\sqrt{n}$ (central limit theorem or CLT [15,16]). The underlying purpose of this measurement is to determine an aspect of p_t fluctuations that is *independent of* event multiplicity *per se*. If n is a random variable, a systematic dependence is introduced into the measured $\langle p_t \rangle$ fluctuation excess through this CLT behavior of the width. To ensure multiplicity independence the basic statistical quantity must be formulated carefully. By normalizing the distribution variable with factor $\sqrt{n}/\sigma_{\hat{p}_t}$, the distribution width of the new variable is unity, independent of n, when fluctuations are purely statistical. The trivial broadening of the $\langle p_t \rangle$ distribution for event ensembles with a finite range of event multiplicities is eliminated. The latter effect can have significant consequences

for relevant event ensembles (p-p, peripheral A-A, and small detector acceptance). This argument explains the variable choice for Fig. 1 as well as the associated numerical analysis described in Sec. IV. For the sake of brevity, this normalized variable will in some cases still be referred to in the text as $\langle p_t \rangle$.

The precision of these data warrants construction of a statistical reference that accurately represents the expected $\langle p_t \rangle$ distribution in the absence of nonstatistical fluctuations. Because of its close connection to the central limit theorem (behavior under n folding noted below), we can compactly and accurately represent the $\langle p_t \rangle$ reference distribution with a gamma distribution [17]. We observe that the measured inclusive p_t distribution is, for present purposes, well approximated by a gamma distribution with folding index $\alpha_0 \equiv \hat{p}_t^2/\sigma_{\hat{p}_t}^2 \approx 2$. Differences between the gamma and inclusive p_t distributions in the higher cumulants due to p_t acceptance cuts and physics correlations are strongly suppressed in the comparison with the distribution in Fig. 1 by inverse powers of event multiplicity and are not significant for central Au-Au collisions.

Because the n folding of a gamma distribution is also a gamma distribution (representing an ensemble of independent n samples of the parent gamma distribution or inclusive p_t distribution), the $\langle p_t \rangle$ reference distribution can be represented by [17]

$$ g_{\bar{n}}(\langle p_t \rangle) = \frac{\alpha_0}{\hat{p}_t} \frac{e^{-\alpha_0 \bar{n} \langle p_t \rangle / \hat{p}_t}}{\Gamma(\alpha_0 \bar{n})} \left(\alpha_0 \bar{n} \frac{\langle p_t \rangle}{\hat{p}_t} \right)^{\alpha_0 \bar{n} - 1}. \quad (2) $$

The corresponding gamma-distribution reference is indicated by the dashed curve in the upper panel of Fig. 1. Parameter values used for this reference curve were determined from the measured inclusive p_t distribution as $\bar{n} = 735 \pm 0.2$, $\hat{p}_t = 535.32 \pm 0.05$ MeV/c, and $\sigma_{\hat{p}_t} = 359.54 \pm 0.03$ MeV/c, obtained from all accepted particles and not corrected for p_t acceptance cuts and inefficiencies.

A reference can also be generated by a Monte Carlo procedure. An ensemble of n-sample reference events is generated with multiplicity distribution similar to the data. A reference event with multiplicity n drawn from that distribution is assembled by performing n random samples from a fixed parent p_t distribution estimated by the interpolated inclusive p_t histogram of all accepted particles from all events in the centrality bin. The resulting Monte Carlo reference distribution is shown in Fig. 1 (upper panel) by the solid curve underlying the dashed gamma reference curve. The agreement is excellent. The broadened distribution (solid curve) underlying the data in the upper panel of Fig. 1 is discussed in Sec. V. All curves are normalized to match the data near the peak value, emphasizing the width comparison, which is the main issue of this paper. We observe a substantial width excess in the data relative to the statistical reference.

The lower panel of Fig. 1 shows the difference between data and gamma reference normalized to Poisson standard deviations in each bin, emphasizing the large statistical significance of the width excess. We observe no significant deviations (bumps) from the broadened distribution in Fig. 1 which might indicate anomalous event classes as expected in some phase-transition scenarios [1]. It is also important to

note that the entire event ensemble contributes to the width increase relative to the statistical reference, i.e., the excess width is not dominated by a subset of problematic events. We note that the distribution in Fig. 1 cannot be corrected for background contamination and tracking inefficiency. The numerical analysis described in the next section allows such corrections.

IV. MEASURES OF NONSTATISTICAL $\langle p_t \rangle$ FLUCTUATIONS

Consistent with the argument presented above about eliminating dependence of fluctuation measures on multiplicity variations within a centrality bin, we characterize the magnitude of nonstatistical $\langle p_t \rangle$ fluctuations by comparing the variance of distribution quantity $\sqrt{n}(\langle p_t \rangle - \hat{p}_t)$ from Fig. 1 to the variance $\sigma_{\hat{p}_t}^2$ of its reference distribution. The difference between these two variances is represented by

$$\Delta\sigma_{p_t:n}^{2\text{(CI)}} \equiv \frac{1}{\varepsilon} \sum_{j=1}^{\varepsilon} n_j [\langle p_t \rangle_j - \hat{p}_t]^2 - \sigma_{\hat{p}_t}^2 \qquad (3)$$

$$\equiv 2\sigma_{\hat{p}_t} \Delta\sigma_{p_t:n}^{\text{(CI)}}, \qquad (4)$$

where ε is the number of events in a centrality bin, j is the event index, n_j is the number of accepted particles in event j, and $\langle p_t \rangle_j$ is the mean p_t of accepted particles in event j. Subscript $p_t{:}n$ emphasizes that this quantity measures variance excess due to fluctuations of p_t *relative to* event-wise fluctuations in multiplicity n (i.e., it is not significantly affected by fluctuations in n itself). Superscript (CI) indicates a *charge-independent* sum over all particles. Difference factor $\Delta\sigma_{p_t:n}^{\text{(CI)}}$ defined in Eq. (4) is approximately equal to $\langle p_t \rangle$ fluctuation measure Φ_{p_t} introduced previously [18,19].

Two issues motivate the definition of fluctuation measure $\Delta\sigma_{p_t:n}^{2\text{(CI)}}$ in Eq. (3): (1) $\langle p_t \rangle$ is the ratio of two random variables—a scalar p_t sum and a multiplicity. Fluctuations in either variable contribute to fluctuations in the ratio. For an uncorrelated system with fluctuating multiplicity, ratio fluctuations go as $1/\sqrt{n}$, producing an apparent nonstatistical contribution to ratio fluctuation measures which are aimed at determining p_t fluctuations. (2) Measures of nonstatistical fluctuations typically involve (at least implicitly) a difference between variances evaluated at two different *scales*, where "scale" in the present context refers to histogram bin sizes (e.g., on η and ϕ). Bins on η and ϕ are denoted respectively by $\delta\eta$ and $\delta\phi$ or generically by δx. The detector acceptance can define one scale, as in this analysis. The other relevant scale, both for the simulated events presented in the preceding section and in the variance measurements presented in Sec. V, is the *single-particle* scale in which the bins are always made small enough such that occupied bins contain a maximum of one particle. In general, the scale is independent of the acceptance where $scale \leqslant acceptance$. The case of variance calculations for arbitrary scale is treated in the Appendix. Scale dependence of variance excess provides important information on the underlying two-particle correlations and is an *essential feature* of any nonstatistical fluctuation measurement such as those presented here, although the importance of this point has not been fully appreciated in this heavy ion context.

In the Appendix we show that the *scale invariance of total variance*, an expression of the central limit theorem, motivates the quantity in Eq. (3). $\Delta\sigma_{p_t:n}^{2\text{(CI)}}(\delta x)$ measures changes in variance stemming from two-particle correlations with characteristic lengths less than the binning scale, δx [16]. As a function of binning scale, $\Delta\sigma_{p_t:n}^{2\text{(CI)}}(\delta x)$ is not dependent on an acceptance *size* (knowledge of its scale dependence may of course be limited by a finite detector acceptance) but can depend on the *absolute position* of the acceptance in momentum space.

Given the definition of Φ_{p_t} [18] and Eq. (3), $\Delta\sigma_{p_t:n}^{2\text{(CI)}} \simeq (\Phi_{p_t} + \sigma_{\hat{p}_t})^2 - \sigma_{\hat{p}_t}^2$, and $\Phi_{p_t} \simeq \Delta\sigma_{p_t:n}^{\text{(CI)}}$ [16]. Difference factor $\Delta\sigma_{p_t:n}^{\text{(CI)}}$ and Φ_{p_t} are therefore comparable between different analyses. Fluctuation measure $\sigma_{p_t,\text{dyn}}^2 \equiv \overline{\langle (p_{t,i} - \hat{p}_t)(p_{t,j} - \hat{p}_t) \rangle_{i \neq j}}$ [20] (overbar denotes event average) is related to $\Delta\sigma_{p_t:n}^{2\text{(CI)}}$ by $\sigma_{p_t,\text{dyn}}^2 \simeq \Delta\sigma_{p_t:n}^{2\text{(CI)}}/(\bar{N}-1)$ ($\bar{N}$ is the mean multiplicity) for approximately constant event-wise multiplicities. Φ_{p_t} and $\sigma_{p_t,\text{dyn}}^2$ may include significant dependence on multiplicity fluctuations in the case of small bin multiplicities (e.g., for any bins within p-p or peripheral A-A events or for small-scale bins within central A-A events). Variance difference $\Delta\sigma_{p_t:n}^{2\text{(CI)}}$ minimizes this dependence compared to the preceding quantities.

In Eqs. (3) and (4) and the Appendix, the summations over particles have ignored charge sign. $\Delta\sigma_{p_t:n}^{2\text{(CI)}}$ is a *charge-independent* (approximately isoscalar) quantity. By separating contributions to Eq. (3) into sums over (+) and (−) charges, a charge-dependent (CD) quantity $\Delta\sigma_{p_t:n}^{2\text{(CD)}}$ can be defined which measures the difference between contributions to $\langle p_t \rangle$ fluctuations from like-sign pairs and unlike-sign pairs. Using explicit charge-sign notation, quantities $\Delta\sigma_{p_t:n}^{2\text{(CI)}}$ and $\Delta\sigma_{p_t:n}^{2\text{(CD)}}$ are defined by

$$\bar{N}(\Delta x)\Delta\sigma_{p_t:n}^{2\text{(CI)}} = \bar{N}(\Delta x)_+ \Delta\sigma_{p_t:n,++}^2$$
$$+ \bar{N}(\Delta x)_- \Delta\sigma_{p_t:n,--}^2$$
$$+ 2\sqrt{\bar{N}(\Delta x)_+ \bar{N}(\Delta x)_-}\, \Delta\sigma_{p_t:n,+-}^2, \quad (5)$$

$$\bar{N}(\Delta x)\Delta\sigma_{p_t:n}^{2\text{(CD)}} = \bar{N}(\Delta x)_+ \Delta\sigma_{p_t:n,++}^2$$
$$+ \bar{N}(\Delta x)_- \Delta\sigma_{p_t:n,--}^2$$
$$- 2\sqrt{\bar{N}(\Delta x)_+ \bar{N}(\Delta x)_-}\, \Delta\sigma_{p_t:n,+-}^2, \quad (6)$$

where $\bar{N}(\Delta x)_\pm$ are the mean multiplicities for $\pm$ charges in acceptance Δx, and $\bar{N}(\Delta x)$ is the mean total multiplicity in Δx. Individual terms in Eqs. (5) and (6) are defined by

$$\Delta\sigma_{p_t:n,ab}^2 \equiv \overline{\sqrt{n_a}(\langle p_t \rangle_a - \hat{p}_{ta})\sqrt{n_b}(\langle p_t \rangle_b - \hat{p}_{tb})}$$
$$- \sigma_{\hat{p}_{t,a}}^2 \delta_{ab}, \quad (7)$$

where subscripts a and b represent the charge sign, $ab = ++, --, +-$ or $-+$, the overbar denotes an average over events, and δ_{ab} is a Kronecker delta. Difference factors $\Delta\sigma_{p_t:n}^{\text{(CI)}}$ and $\Delta\sigma_{p_t:n}^{\text{(CD)}}$ (approximately isoscalar and isovector, respectively) reported in the following sections are defined by

$$\Delta\sigma_{p_t:n}^{2\text{(CI)}} = 2\sigma_{\hat{p}_t} \Delta\sigma_{p_t:n}^{\text{(CI)}} \qquad (8)$$

$$\Delta\sigma_{p_t:n}^{2\text{(CD)}} = 2\sigma_{\hat{p}_t} \Delta\sigma_{p_t:n}^{\text{(CD)}}. \qquad (9)$$
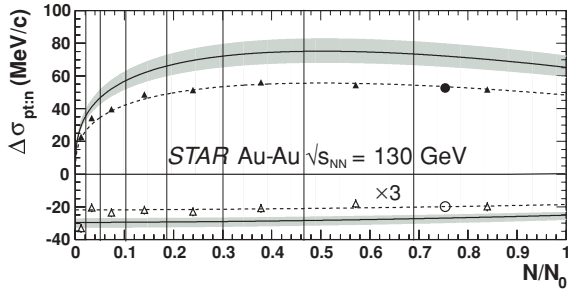
FIG. 2. (Color online) Mean-p_t difference factors $\Delta\sigma_{p_t:n}^{(CI)}$ and $\Delta\sigma_{p_t:n}^{(CD)}$ for 205k minimum-bias Au-Au events at $\sqrt{s_{NN}} = 130$ GeV vs relative multiplicity N/N_0 [14], which is approximately $N_{part}/N_{part,max}$, the relative fraction of participant nucleons [21]. Charge-independent (solid triangular points) and charge-dependent (open triangular points, multiplied by 3 for clarity) difference factors include statistical errors only (smaller than symbols). Parametrizations (dashed curves), extrapolation of parametrizations to true primary particle number (solid curves), and systematic uncertainties (bands) are discussed in the text. Difference factors for the 15% most-central collision events are shown by the solid circle and open circle symbols.

V. RESULTS

We apply Eqs. (5)–(9) to central collisions and to a minimum-bias ensemble. In all cases, charge symmetry $\Delta\sigma_{p_t:n,++}^2 \simeq \Delta\sigma_{p_t:n,--}^2$ is observed within errors. For the 15% most-central events and full acceptance, we obtain difference factors $\Delta\sigma_{p_t:n}^{(CI)} = 52.6 \pm 0.3$ (stat) MeV/c and $\Delta\sigma_{p_t:n}^{(CD)} = -6.6 \pm 0.6$ (stat) MeV/c (respectively, the solid and open circular data symbols in Fig. 2). Charge-independent values of Φ_{p_t} and $\sigma_{p_t,dyn}^2$ for the same data are respectively 52.6 ± 0.3 (stat) MeV/c and 52.3 ± 0.3 (stat) (MeV/c)^2 (note units). Dependence on multiplicity fluctuations is negligible for this full-acceptance, 15% most-central collision ensemble.

The experimental value $\Delta\sigma_{p_t:n}^{(CI)} = 52.6$ MeV/c was used to determine the solid curves underlying the data histogram in the two panels of Fig. 1 by raising the reference gamma distribution in Eq. (2) to the power $\sigma_{\hat{p}_t}^2/(\sigma_{\hat{p}_t}^2 + \Delta\sigma_{p_t:n}^{2(CI)})$. This procedure, which would be exact for a Gaussian distribution, increases the variance of the modified gamma distribution to the numerical value obtained from the data, preserves the mean, and agrees well with the relative peak heights of the data in the lower half of Fig. 1. The comparison in Fig. 1 then demonstrates that $\Delta\sigma_{p_t:n}^{(CI)}$ provides an excellent description of the event-wise $\langle p_t \rangle$ distribution and its fluctuation excess. The corresponding r.m.s. width increase relative to the reference is 13.7 ± 0.1(stat) ± 1.3(syst)%. When extrapolated to 100% of primary hadrons and no backgrounds, $\Delta\sigma_{p_t:n}^{(CI,CD)}$ was estimated to be a factor of 1.26 larger in magnitude for the 15% most-central events, resulting in a corrected charge-independent r.m.s. width increase of 17 ± 2(syst)%.

Difference factors were also determined for eight centrality classes defined for the 205k minimum-bias events described in Sec. II. Measured values of $\Delta\sigma_{p_t:n}^{(CI)}$ and $\Delta\sigma_{p_t:n}^{(CD)}$ are shown in Fig. 2 by the upper and lower set of data symbols for CI and CD, respectively, plotted for each centrality class, vs its mean multiplicity $\bar{N}$ in $|\eta| \leqslant 0.5$ (Sec. II) relative to N_0, the

TABLE I. Centrality dependences of the measured charge-independent (CI) and charge-dependent (CD) difference factors $\Delta\sigma_{p_t:n}^{(CI)}$ and $\Delta\sigma_{p_t:n}^{(CD)}$ plus the corresponding values extrapolated to 100% tracking efficiency. Uncertainties in the latter are $\pm 12\%$ and dominated by systematics, as discussed in the text.

Centrality			$\Delta\sigma_{p_t:n}^{(CI)}$ (MeV/c)		$\Delta\sigma_{p_t:n}^{(CD)}$ (MeV/c)	
$\bar{N}/N_0$	$\frac{\sigma}{\sigma_{tot}}(\%)$[a]	N_{part}[b]	Data[c]	Ext.[d]	Data[c]	Ext.[d]
0.012	87–76	8.9	22.8	26.8	−11.1	−13.0
0.033	76–65	19	34.3	40.4	−6.9	−8.1
0.073	65–54	36	39.6	46.8	−7.9	−9.3
0.14	54–43	64	48.7	57.9	−7.4	−8.8
0.24	43–33	102	51.3	61.4	−7.7	−9.2
0.38	33–22	153	56.1	68.0	−7.0	−8.5
0.57	22–11	224	54.4	66.9	−6.0	−7.4
0.84	11–0	320	51.8	65.1	−6.6	−8.3

[a]Fraction of total hadronic inelastic cross section ranges in percent; values are $\pm 2\%$ uncertain [14].
[b]Estimates in [14] were interpolated to centrality bins used here.
[c]Statistical errors are typically ± 0.5 MeV/c; systematic errors are $\pm 9\%$.
[d]Difference factors extrapolated to 100% tracking efficiency and no secondary particle contamination.

minimum-bias multiplicity distribution endpoint [21] where $N_0 = 520 \pm 5$. Data are listed in Table I. Plotted points, including statistical errors only (typically ± 0.5 MeV/c), were fitted with parametrizations (dashed curves) which were then extrapolated by amounts varying from 1.17 to 1.26 (for peripheral to central events respectively) to produce estimates for 100% of primary charged hadrons (solid curves). $\Delta\sigma_{p_t:n}^{(CI)}$ has a very significant nonmonotonic dependence on centrality, but with no sharp structure. $\Delta\sigma_{p_t:n}^{(CD)}$ is significantly negative and approximately independent of centrality. Φ_{p_t} and $\sigma_{p_t,dyn}^2(\bar{N} - 1)/2\sigma_{\hat{p}_t}$ agree with $\Delta\sigma_{p_t:n}^{(CI)}$ within statistical errors for the upper six centrality classes, but both differ from $\Delta\sigma_{p_t:n}^{(CI)}$ and each other by much more than statistical uncertainty for the two most peripheral bins, as expected from their dependencies on multiplicity fluctuations.

Systematic errors from uncertainty in two-track inefficiency, primary-vertex transverse position uncertainty, TPC drift speed/time-offset uncertainty, and conversion electron contamination were estimated by Monte Carlo [22] as less than 4% of reported values. Stability of reported results against primary-vertex longitudinal position variation, momentum resolution, and TPC central membrane track crossing was determined to be 5% of stated values. Systematic effects due to possible time dependence in detector performance and efficiency were studied by analyzing sequential run blocks which were determined to be consistent within statistical error. Systematic error contributions due to azimuthal anisotropy in the event-wise primary particle distribution ($\cos[2(\phi - \Psi_R)]$ assumed where Ψ_R is the event-wise reaction plane angle) combined with nonuniform azimuthal tracking efficiency were determined to be less than 1% of reported values using ϕ-dependent track cuts and measured efficiency maps. Non-primary background ($\sim 7\%$) [14] added $\pm 7\%$ systematic error

due to uncertainty in its correlation content. Total systematic uncertainty for the $\Delta\sigma_{p_t:n}^{(CI)}$ and $\Delta\sigma_{p_t:n}^{(CD)}$ data in Fig. 2 and Table I is $\pm 9\%$. Additional systematic error in extrapolation of $\Delta\sigma_{p_t:n}^{(CI)}$ and $\Delta\sigma_{p_t:n}^{(CD)}$ to 100% of primary particles ($\pm 8\%$) is dominated by uncertainty in the actual primary particle yield [14]. Total uncertainty in extrapolated values is about $\pm 12\%$ (shaded bands in Fig. 2). Systematic error in the most peripheral bin is larger by an additional $\sim \pm 1$ MeV/c due to possible primary-vertex reconstruction bias. Analyses of 30 000 central HIJING Au-Au collision events both with and without STAR acceptance and event reconstruction effects yield consistent results for $\Delta\sigma_{p_t:n}^{(CI)}$ to within the statistical error ($\sim 10\%$) for these simulated events, which is well within our estimated systematic error.

Data in Fig. 2 and Table I were not corrected for two-track inefficiencies, which would increase all results in a positive sense by up to 3 MeV/c. Variations ($\approx 10\%$) in $\hat{p}_t$ and $\sigma_{\hat{p}_t}^2$ with collision centrality were accommodated by independent analyses in small centrality bins. Monte Carlo [22] estimates indicate that combined corrections for quantum (Hanbury Brown and Twiss) and Coulomb correlations [10], resonance (ρ^0, ω) decays, and $\hat{p}_t$ centrality dependence (i.e., well known physical effects) would *increase* the absolute magnitudes of all data in Fig. 2 and Table I by as much as ≈ 6 MeV/c. Quantum and Coulomb correlations and resonance decays originate in the final stage of the collision evolution and are not the main object of this study. Correcting $\Delta\sigma_{p_t:n}^{(CI)}$ for two-track inefficiencies plus the preceding effects (not done for the data shown in Fig. 2 and Table I) would cause the overall magnitude to increase by about 7 MeV/c. Similarly, corrections to $\Delta\sigma_{p_t:n}^{(CD)}$ would cause it to become more negative by about 4 MeV/c. We conclude that the negative values of $\Delta\sigma_{p_t:n}^{(CD)}$ are physically significant and cannot be explained by conventional effects such as Coulomb interactions, resonance decays, or tracking inefficiencies.

VI. EXPERIMENT COMPARISONS

CERN Super Proton Synchrotron (SPS) charge-independent Φ_{p_t} measurements with a 158 GeV per nucleon Pb beam on fixed heavy ion targets ($\sqrt{s_{NN}} \approx 17.3$ GeV) include values 0.6 ± 1.0 MeV/c for central collisions on Pb nuclei with $\bar{N} \simeq 270$ in CM pion rapidity interval $1.1 \leqslant y_{\pi,\text{cm}} \leqslant 2.6$ (experiment NA49) [19] and $3.3 \pm 0.7^{+1.8}_{-1.6}$ MeV/c for central collisions on Au nuclei with $\bar{N} \simeq 162$ in laboratory pseudorapidity interval $2.2 \leqslant \eta_{\text{lab}} \leqslant 2.7$ (midpseudorapidity region) from the CERES experiment [23]. STAR measures $\Delta\sigma_{p_t:n}^{(CI)} = 14 \pm 2$ MeV/$c \simeq \Phi_{p_t}$ for $\bar{N} \sim 180$ when restricted to the CERES η acceptance scale [23]. All three measurements were corrected for small-scale correlations and two-track inefficiencies. In a following analysis [24] of the 158 GeV per nucleon Pb-Pb fixed target collision data, experiment NA49 reported charge-independent Φ_{p_t} measurements for all charged particles in rapidity interval $1.1 \leqslant y_{\pi,\text{cm}} \leqslant 2.6$ (pion mass assumed) as a function of centrality. Φ_{p_t} values were found to monotonically decrease from $7.2 \pm 0.7 \pm 1.6$ MeV/c for most-peripheral to $1.4 \pm 0.8 \pm 1.6$ MeV/c for most-central collisions. Corrections for finite two-track resolution were included; however, the contributions of quantum and Coulomb

small-scale correlations, estimated to be 5 ± 1.5 MeV/c [19], remain. Quantity $\Sigma_{p_t} \equiv \sqrt{\Delta\sigma_{p_t:n}^{2(CI)}/\bar{N}\hat{p}_t^2}$ was also reported by the CERES experiment [23] with a magnitude approximately half that at STAR. Results from STAR for $\Delta\sigma_{p_t:n}^{(CI)}$ at RHIC energy represent a striking increase over SPS results and markedly different centrality dependence. In contrast, STAR's measurement of $\Delta\sigma_{p_t:n}^{(CD)}$ is not significantly different from the NA49 result -8.5 ± 1.5 MeV/c in $1.1 \leqslant y_{\pi,\text{cm}} \leqslant 2.6$ [25].

The PHENIX experiment at RHIC reports charge-independent $\Phi_{p_t} \approx 6 \pm 6$ (syst) MeV/c for the uppermost 5% central Au-Au collision events at $\sqrt{s_{NN}} = 130$ GeV within their acceptance: $|\eta| < 0.35$ and $\Delta\phi = 58.5°$ [26]. This STAR analysis restricted to the PHENIX (η, ϕ) acceptance scale obtained $\Delta\sigma_{p_t:n}^{(CI)} \sim 9 \pm 1$ MeV/c. That value is greater than would be expected from naive scaling from the STAR full-acceptance scale ($\Delta\eta = 2, \Delta\phi = 2\pi$) to the PHENIX acceptance scale ($\Delta\eta = 0.7, \Delta\phi = 58.5°$) [27]. The enhanced value for $\Delta\sigma_{p_t:n}^{(CI)}$ relative to linear scale dependence is observed to result from substantial nonlinear azimuth-scale ($\delta\phi$) dependence of $\langle p_t \rangle$ fluctuations (mainly a $\cos[2(\phi - \Psi_R)]$ term).

PHENIX also reports nonzero nonstatistical $\langle p_t \rangle$ fluctuations for Au-Au collisions at $\sqrt{s_{NN}} = 200$ GeV using quantity F_{p_t} [28] (proportional to Φ_{p_t} and $\Delta\sigma_{p_t:n}^{(CI)}$) and acceptance scales $\Delta\eta = 0.7$ at midrapidity and $\Delta\phi = 180°$ in two approximately opposed 90° spectrometer arms. $\langle p_t \rangle$ fluctuations for central collisions at 200 GeV (with two opposed spectrometer arms) are observed to be similar to those at 130 GeV (with one spectrometer arm) assuming linear dependence on azimuth scale [27].

Analysis of the dependence of $\Delta\sigma_{p_t:n}^{(CI,CD)}$ on the upper p_t acceptance cut indicates significant contribution from particles with $p_t > 0.6$ GeV/c. Subsequent studies of like-sign and unlike-sign two-particle correlations on transverse momentum space [29] for these data confirm that much of the observed fluctuations result from correlation excess for $p_t > 0.6$ GeV/c. The larger magnitude of unlike-sign correlations relative to like-sign at higher $p_t > 0.6$ GeV/c also results in $\Delta\sigma_{p_t:n}^{(CD)} < 0$. These results implicate semihard scattering in the initial stage of Au-Au collisions as a possible mechanism contributing to $\Delta\sigma_{p_t:n}^{(CI)}$ and $\Delta\sigma_{p_t:n}^{(CD)}$. Strong dependence of F_{p_t} on the upper p_t acceptance was also reported by the PHENIX experiment [28]. It is therefore of interest to examine the predictions of available theoretical collision models which include hard parton scattering and/or hadronic rescattering.

VII. MODEL PREDICTIONS

HIJING [5], which incorporates p-p soft scattering and longitudinal color-string fragmentation phenomenology plus hard parton scattering and fragmentation coupled to a Glauber model of A-A collision geometry, predicts a range of $\Delta\sigma_{p_t:n}^{(CI)}$ up to only one-half the observed values in Fig. 2. HIJING predictions include (1) jet production enabled but without jet quenching (produces maximum fluctuations but still only one-half the measured values); (2) jet production and jet quenching both enabled (variance excess reduced by about half); and (3) no jet production (even smaller magnitude). In addition to underpredicting $\Delta\sigma_{p_t:n}^{(CI)}$ magnitudes, HIJING

does not reproduce the observed strong centrality dependence of the data or the nonmonotonic behavior for the more central collisions; its predictions are instead approximately independent of centrality.

Other collision models differ in their treatment of lower p_t (soft) particle production, rescattering, and resonances, but they do not include semihard parton scattering. RQMD [30] without hadronic rescattering, predicts that $\Delta\sigma_{p_t:n}^{(CI)}$ increases monotonically with centrality, reaching only half the observed value for central RHIC collisions. Initial studies of scale dependence indicate that the main contribution in the RQMD model is from resonance decays and not minijets as for HIJING. Φ_{p_t} predictions from UrQMD for Au-Au collisions at $\sqrt{s_{NN}} = 200$ GeV [31] indicate results similar to RQMD and also reveal strong reduction of Φ_{p_t} when hadronic rescattering is included. RQMD and UrQMD predictions for $\Delta\sigma_{p_t:n}^{(CI)}$ without hadronic rescattering constitute the upper limit for those models. The quark-gluon string model (QGSM) for Pb-Pb central collisions at $\sqrt{s_{NN}} = 200$ GeV, when linearly extrapolated to the STAR acceptance scale, predicts $\Delta\sigma_{p_t:n}^{(CI)} \sim 10$ MeV/c [32], which is significantly less than the STAR measurement.

VIII. DISCUSSION

These fluctuation measurements, restricted to hadrons at lower p_t (<2 GeV/c), indicate that even central Au-Au collisions at RHIC are not fully equilibrated because $\Delta\sigma_{p_t:n}^{(CI,CD)}$ would vanish for ensembles of fully equilibrated events (except for the relatively small contributions from quantum and Coulomb correlations and resonance decays). Instead, Au-Au collision events at RHIC remain highly structured, with respect to nonstatistical $\langle p_t \rangle$ fluctuations, as evidenced by the strong dependence on the upper p_t acceptance. This result conflicts with assumptions underlying hydrodynamic and statistical (thermal) models conventionally applied to RHIC collisions. We observe no evidence of critical fluctuations associated with a possible phase transition. The quantity $\Delta\sigma_{p_t:n}^{(CI)}$ used in this analysis quantifies the substantial differences between Au-Au collisions and simple models based on independent superposition of p-p collisions. We have demonstrated that the observed charge-independent and charge-dependent nonstatistical fluctuations cannot be explained in terms of final-state quantum and Coulomb correlations and resonance decays or in terms of experimental effects such as two-track inefficiencies and time dependences of experimental apparatus.

The observed strong energy dependence of $\Delta\sigma_{p_t:n}^{(CI)}$ from SPS to RHIC and the failure of conventional theoretical models to describe these new RHIC fluctuation data indicate that significant new dynamical mechanisms play a role in Au-Au collisions at RHIC, mechanisms that substantially affect the correlation structure of final-state transverse momentum. The increase of $\Delta\sigma_{p_t:n}^{(CI)}$ with p_t upper limit, combined with apparent saturation and even reduction of $\Delta\sigma_{p_t:n}^{(CI)}$ for the more central Au-Au collisions, suggests that semihard parton scattering and subsequent dissipation of parton momentum by coupling to an increasingly dense, possibly colored medium may account for these observations. Detailed studies of correlation structure in

both transverse and longitudinal momentum components will be reported in the near future [7,29,33].

IX. CONCLUSIONS

This first large-acceptance measurement of $\langle p_t \rangle$ fluctuations at RHIC reveals intriguing deviations from a statistical reference. We observe a $13.7 \pm 1.4\%$ (stat+syst) r.m.s. fractional excess of charge-independent fluctuations in $\sqrt{n}(\langle p_t \rangle - \hat{p}_t)$ [$17 \pm 2\%$ (stat+syst) when extrapolated to 100% of primary charged hadrons in the STAR acceptance] for the 15% most-central events which varies smoothly and nonmonotonically with centrality. This observation of strong nonstatistical $\langle p_t \rangle$ fluctuations demonstrates that RHIC events are not fully equilibrated, even in the lower p_t sector for central events, contradicting a basic assumption of hydrodynamic and statistical models. There is no significant evidence for anomalous event classes as might be expected from critical fluctuations. Comparisons with SPS experiments indicate that charge-independent fluctuations are qualitatively larger at RHIC, whereas charge-dependent fluctuations are not. A PHENIX result at 130 GeV for charge-independent fluctuations, compatible with zero within their systematic error, is consistent with a significant nonzero STAR measurement restricted to the PHENIX acceptance. Based upon studies of the higher p_t contribution and various model comparisons, we speculate that these fluctuations may be a consequence of semihard initial-state scattering (minijets) followed by parton cascade in the early stage of the Au-Au collision which is not fully equilibrated prior to kinetic decoupling [34]. Such strong fluctuations have not been observed previously in heavy ion collisions and are at present unexplained by theory, thus pointing to the possibility of new, or perhaps unexpected dynamical processes occuring at RHIC. Identification of the dynamical source(s) of these nonstatistical fluctuations is underway [29] and will continue to be studied in the future.

APPENDIX

In this appendix the *total variance* is defined. The *scale invariance* of total variance, an alternative statement of the central limit theorem [15,16], then motivates the definition of fluctuation measure $\Delta\sigma_{p_t:n}^{2(CI)}$ used in this analysis.

A detector acceptance $(\Delta\eta, \Delta\phi)$ (generically Δx) on axial momentum space (η, ϕ) can be divided into bins of size $(\delta\eta, \delta\phi)$ (generically δx). Each bin then contains an event-wise scalar p_t sum

$$p_{t,\alpha}(\delta x) \equiv \sum_{i=1}^{n_\alpha(\delta x)} p_{t,\alpha i}, \qquad (A1)$$

where α is a bin index and $n_\alpha(\delta x)$ is the event-wise multiplicity in bin α. Fluctuations in $p_{t,\alpha}(\delta x)$ *relative to* $n_\alpha(\delta x)$ could be measured by the variance of the ratio $\langle p_t \rangle_\alpha = p_{t,\alpha}(\delta x)/n_\alpha(\delta x)$. However, to minimize contributions from event-wise and *bin-wise* variations in $n_\alpha(\delta x)$ (a source of systematic error) we instead compute the *total variance* of difference $p_{t,\alpha}(\delta x) - n_\alpha(\delta x)\hat{p}_t$, defined by

$$\Sigma^2_{p_t:n}(\Delta x, \delta x) \equiv \overline{\sum_{\alpha=1}^{M(\Delta x, \delta x)} (p_{t,\alpha}(\delta x) - n_\alpha(\delta x)\,\hat{p}_t)^2}, \quad (A2)$$

where $M(\Delta x, \delta x)$ is the event-wise number of *occupied* bins of size δx in acceptance Δx and the overbar denotes an average over all events. Typically $M(\Delta x, \delta x) = \Delta x / \delta x$, a constant for all events except when $\delta x \ll \Delta x$ and some bins are unoccupied.

For the analysis described in this paper, we are interested in two limits of Eq. (A2), the acceptance scale $\delta x = \Delta x$ with $M = 1$, and a single-particle scale $\delta x \ll \Delta x$ such that each occupied (η, ϕ) bin contains a single particle, with $M \to n(\Delta x) \equiv N(\Delta x)$, the event-wise total multiplicity in the acceptance. For a collection of reference events (cf. Sec. III) obtained by independent p_t sampling from a fixed parent distribution (also referred to here as CLT conditions), quantity $\Sigma^2_{p_t:n}(\Delta x, \delta x)$ is independent of bin size δx. We illustrate this *scale invariance* under CLT conditions for the above two limits and for arbitrary scale δx as follows.

In the single-particle scale limit, each occupied bin contains only one particle, and the bin index is equivalent to a particle index: $p_{t,\alpha}(\delta x) \to p_{t,i}$ (transverse momentum of particle i) and $n_\alpha(\delta x) \to 1$. $\Sigma^2_{p_t:n}(\Delta x, \delta x)$ then has the limit

$$\Sigma^2_{p_t:n}(\Delta x, \delta x \ll \Delta x) \to \bar{N}(\Delta x)\sigma^2_{\hat{p}_t}, \qquad (A3)$$

where $\bar{N}(\Delta x)$ is the mean total event multiplicity, and the variance of the inclusive p_t distribution is explicitly $\sigma^2_{\hat{p}_t} = \overline{\sum_{i=1}^{N(\Delta x)} (p_{t,i} - \hat{p}_t)^2}/\bar{N}(\Delta x)$. In the limit $\delta x \to \Delta x$, $M(\Delta x, \delta x) \to 1$, the event-wise single-bin occupancy is $N(\Delta x)$, and $\Sigma^2_{p_t:n}(\Delta x, \delta x)$ becomes

$$\Sigma^2_{p_t:n}(\Delta x, \delta x = \Delta x) = \sum_{N(\Delta x)} p_N N(\Delta x)^2 \sigma^2_{\langle p_t \rangle_N}, \qquad (A4)$$

where the sum includes all values of event multiplicity $N(\Delta x)$ represented in the event ensemble, $p_N \equiv \varepsilon_N/\varepsilon$ is the fraction of events in the ensemble with multiplicity $N(\Delta x)$, and $\sigma^2_{\langle p_t \rangle_N} \equiv \overline{(\langle p_t \rangle_N - \hat{p}_t)^2}$ is the variance of the $\langle p_t \rangle$ distribution for the subset of events with multiplicity $N(\Delta x)$. If CLT conditions

apply, then

$$\Sigma^2_{p_t:n}(\Delta x, \Delta x) \overset{\text{(CLT)}}{=} \sum_N p_N N(\Delta x)\sigma^2_{\hat{p}_t}$$
$$= \bar{N}(\Delta x)\sigma^2_{\hat{p}_t}, \qquad (A5)$$

where CLT relation $\sigma^2_{\langle p_t \rangle_N} = \sigma^2_{\hat{p}_t}/N(\Delta x)$ was invoked. The equivalence under CLT conditions of $\Sigma^2_{p_t:n}(\Delta x, \delta x)$ for these two limiting scale values is thus established.

Generalizing the latter argument, the total variance at arbitrary scale δx in Eq. (A2) can be reexpressed as

$$\Sigma^2_{p_t:n}(\Delta x, \delta x) = \overline{\sum_{\alpha=1}^{M(\Delta x, \delta x)} n_\alpha^2(\delta x)(\langle p_t \rangle_\alpha - \hat{p}_t)^2}$$
$$= M(\Delta x, \delta x) \sum_{n(\delta x)} p_n n^2(\delta x)\sigma^2_{\langle p_t \rangle_n}, \qquad (A6)$$

where sums over events and bins were rearranged as sums over bin-wise multiplicity $n(\delta x)$ and over bins α which have that value of multiplicity, p_n is the fraction of bins in the event ensemble with multiplicity $n(\delta x)$, and $\sigma^2_{\langle p_t \rangle_n}$ is the variance of $\langle p_t \rangle - \hat{p}_t$ within that subset of bins

$$\sigma^2_{\langle p_t \rangle_n} \equiv \overline{(\langle p_t \rangle_n - \hat{p}_t)^2}. \qquad (A7)$$

The overbar in Eq. (A7) indicates an average over all bins in the event ensemble with multiplicity n. For CLT conditions $\sigma^2_{\langle p_t \rangle_n} = \sigma^2_{\hat{p}_t}/n(\delta x)$ for any n, and since $M(\Delta x, \delta x)\bar{n}(\delta x) = \bar{N}(\Delta x)$, Eq. (A6) therefore becomes

$$\Sigma^2_{p_t:n}(\Delta x, \delta x) = \bar{N}(\Delta x)\sigma^2_{\hat{p}_t}, \qquad (A8)$$

which demonstrates the general scale invariance of $\Sigma^2_{p_t:n}(\Delta x, \delta x)$ for CLT conditions.

Deviations from central limit conditions signal the presence of two-particle correlations (e.g., p_t samples are not independent). The total variance is then no longer scale invariant, and its scale dependence reflects the detailed structure of those correlations. We therefore define a *total variance difference* between arbitrary scales δx_1 and δx_2, where $\delta x_1 < \delta x_2$, as

$$\Delta\Sigma^2_{p_t:n}(\Delta x, \delta x_1, \delta x_2) \equiv \Sigma^2_{p_t:n}(\Delta x, \delta x_2) - \Sigma^2_{p_t:n}(\Delta x, \delta x_1), \qquad (A9)$$

where $\Delta\Sigma^2_{p_t:n}(\Delta x, \delta x_1, \delta x_2) = 0$ if CLT conditions apply in the scale interval $[\delta x_1, \delta x_2]$.

The total variance difference depends by construction on the detector acceptance (and on the collision system or participant number). We can remove those dependences in several ways, which choice depends on the physical mechanisms producing the correlations. For this application, we divide by the total multiplicity in the acceptance to obtain a fluctuation measure *per final-state particle*.

If CLT conditions are approximately valid, $n(\delta x)\sigma^2_{\langle p_t \rangle_n}$ in Eq. (A6) is nearly constant and can be removed from the weighted summation over n, resulting in

$$\Sigma^2_{p_t:n}(\Delta x, \delta x) \simeq \bar{N}(\Delta x)\overline{n(\delta x)(\langle p_t \rangle - \hat{p}_t)^2}, \qquad (A10)$$

a factorized form in which acceptance and scale dependences are separated. The total variance difference for $\delta x_2 = \delta x$ and

$\delta x_1 \ll \Delta x$ is then given by

$$\Delta\Sigma^2_{p_t:n}(\Delta x, \delta x_1 \ll \Delta x, \delta x)$$
$$\simeq \bar{N}(\Delta x)\left[\overline{n(\delta x)(\langle p_t\rangle - \hat{p}_t)^2} - \sigma^2_{\hat{p}_t}\right]$$
$$\equiv \bar{N}(\Delta x)\Delta\sigma^2_{p_t:n}(\delta x), \tag{A11}$$

combining Eqs. (A3) and (A10). In Eqs. (A10) and (A11), the overbar denotes an event-wise average over occupied bins and an average over all events. The $\langle p_t\rangle$ fluctuation excess measure $\Delta\sigma^{2\text{(CI)}}_{p_t:n}$ in Eq. (3) is thus identified as the total variance difference in Eq. (A11) *per final-state particle*, evaluated at the acceptance scale $\delta x = \Delta x$.

[1] R. Stock, Nucl. Phys. **A661**, 282c (1999); H. Heiselberg, Phys. Rep. **351**, 161 (2001).

[2] M. Stephanov, K. Rajagopal, and E. Shuryak, Phys. Rev. D **60**, 114028 (1999).

[3] A. Dumitru and R. Pisarski, Phys. Lett. **B504**, 282 (2001).

[4] M. Gaździcki, A. Leonidov, and G. Roland, Eur. Phys. J. C **6**, 365 (1999).

[5] X.-N. Wang and M. Gyulassy, Phys. Rev. D **44**, 3501 (1991).

[6] H. R. Schmidt and J. Schukraft, J. Phys. G **19**, 1705 (1993).

[7] J. Adams *et al.* (STAR Collaboration), nucl-ex/0406035.

[8] K. Adcox *et al.* (PHENIX Collaboration), Phys. Rev. Lett. **89**, 082301 (2002).

[9] J. Adams *et al.* (STAR Collaboration), Phys. Rev. Lett. **90**, 172301 (2003).

[10] C. Adler *et al.* (STAR Collaboration), Phys. Rev. Lett. **87**, 082301 (2001).

[11] B. Andersson, G. Gustafson, G. Ingelman, and T. Sjöstrand, Phys. Rep. **97**, 31 (1983).

[12] J. Whitmore, Phys. Rep. **27**, 187 (1976).

[13] K. H. Ackermann *et al.* (STAR Collaboration), Nucl. Instrum. Methods A **499**, 624 (2003); see other STAR papers in volume A 499.

[14] C. Adler *et al.* (STAR Collaboration), nucl-ex/0311017; Phys. Rev. Lett. **87**, 112303 (2001); **89**, 202301 (2002); J. Adams *et al.* (STAR Collaboration), submitted to Phys. Rev. C.

[15] E. U. Condon and H. Odishaw, in *Handbook of Physics* (McGraw-Hill, New York, 1967), 2nd ed., Chap. 12, pp. 177–178.

[16] T. A. Trainor, hep-ph/0001148.

[17] M. J. Tannenbaum, Phys. Lett. **B498**, 29 (2001).

[18] M. Gaździcki and St. Mrówczyński, Z. Phys. C **54**, 127 (1992).

[19] H. Appelshäuser *et al.* (NA49 Collaboration), Phys. Lett. **B459**, 679 (1999).

[20] S. A. Voloshin, V. Koch, and H. G. Ritter, Phys. Rev. C **60**, 024901 (1999).

[21] N_0 is the half-max point at the end of the minimum-bias distribution plotted as $d\sigma/dN_{\text{ch}}^{1/4}$, and is an estimator on N for the maximum number of participant nucleons, in which case $N_{\text{part}}/N_{\text{part,max}} \simeq N/N_0$ within 4%.

[22] R. Ray and R. Longacre, nucl-ex/0008009.

[23] D. Adamová *et al.* (CERES Collaboration), Nucl. Phys. **A727**, 97 (2003).

[24] T. Anticic *et al.* (NA49 Collaboration), Phys. Rev. C **70**, 034902 (2004).

[25] J. G. Reid, Ph.D. thesis, University of Washington (2002), nucl-ex/0302001.

[26] K. Adcox *et al.* (PHENIX Collaboration), Phys. Rev. C **66**, 024901 (2002).

[27] The assumption underlying this naive scaling is that the correlation range is much greater than the scale, such that $\Delta\sigma^{\text{(CI)}}_{p_t:n}$ is proportional to $\delta\eta$ and $\delta\phi$.

[28] S. S. Adler *et al.* (PHENIX Collaboration), Phys. Rev. Lett. **93**, 092301 (2004).

[29] J. Adams *et al.* (STAR Collaboration), nucl-ex/0408012.

[30] H. Sorge, H. Stöcker, and W. Greiner, Nucl. Phys. **A498**, 567c (1989); Ann. Phys. (NY) **192**, 266 (1989).

[31] S. A. Bass *et al.*, Prog. Part. Nucl. Phys. **41**, 255 (1998); M. Bleicher, unpublished, 1999.

[32] A. Capella, E. G. Ferreiro, and A. B. Kaidalov, Eur. Phys. J. C **11**, 163 (1999).

[33] J. Adams *et al.* (STAR Collaboration), nucl-ex/0411003.

[34] Q. Liu and T. A. Trainor, Phys. Lett. **B567**, 184 (2003).